



Pergamon

Acta Materialia 50 (2002) 2331–2341



www.actamat-journals.com

# Optimization of grain boundary character distribution for intergranular corrosion resistant 304 stainless steel by twin-induced grain boundary engineering

M. Shimada \*, H. Kokawa, Z.J. Wang, Y.S. Sato, I. Karibe

*Department of Materials Processing, Graduate School of Engineering, Tohoku University, Aoba-yama 02, Sendai 980-8579, Japan*

Received 15 November 2001; received in revised form 31 January 2002; accepted 1 February 2002

## Abstract

The effects of process parameters, pre-strain, annealing temperature, time, etc. on grain boundary character distribution (GBCD) and intergranular corrosion in thermomechanical treatment were examined during grain boundary engineering of type 304 austenitic stainless steel. Slight pre-strain annealing at a relatively low temperature resulted in excellent intergranular corrosion resistance due to optimized GBCD, i.e. the uniform distribution of a high frequency of coincidence site lattice boundaries and consequent discontinuity of random boundary network in the material. The optimum distribution can be formed by introduction of low energy segments on migrating random boundaries during twin emission and boundary–boundary reactions in the grain growth without generation of new random boundaries. © 2002 Acta Materialia Inc. Published by Elsevier Science Ltd. All rights reserved.

*Keywords:* Grain boundaries; Corrosion; Grain boundary engineering; Austenite

## 1. Introduction

Intergranular corrosion of austenitic stainless steels is a conventional and momentous problem during welding and high temperature use. One of the major reasons for such intergranular corrosion is so-called sensitization, i.e. chromium depletion due to chromium carbide precipitation at grain boundaries. Conventional methods for preventing sensitization of austenitic stainless steels include reduction of carbon

content in the material, stabilization of carbon atoms as non-chromium carbides by the addition of titanium, niobium or zirconium, local solution-heat-treatment by laser beam, etc. These methods, however, are not without drawbacks.

Recent grain boundary structure studies have demonstrated that grain boundary phenomena (grain boundary diffusion [1], precipitation [2,3], corrosion [4,5], etc.) strongly depend on the crystallographic nature and atomic structure of the grain boundary [6]. Grain boundary structure dependence of intergranular carbide precipitation and corrosion has been reported in nickel [7], nickel alloy [8] and austenitic stainless steels [9,10]. Time–temperature–precipitation curve

\* Corresponding author. Tel: +81-22-217-7353; fax: +81-22-217-7352.

*E-mail address:* shimada@stu.material.tohoku.ac.jp (M. Shimada).

reported for austenitic stainless steels have indicated that twin boundaries are not susceptible to either carbide precipitation nor corrosion, because the atomic structure is highly regular and coherent as compared with those of other high angle grain boundaries [11,12]. Trillo and Murr [13,14] have reported a remarkable resistance of coherent twin boundary to carbide precipitation because of extreme low boundary energy. This suggests that each grain boundary has its own sensitivity to sensitization depending on the nature and structure of the grain boundary.

Grain boundaries with low- $\Sigma$  coincidence site lattices (CSLs) are immune to intergranular corrosion [7–10,15,16]. Watanabe introduced the concept of ‘grain boundary design and control’, which involves a desirable grain boundary character distribution (GBCD), including high frequency of CSL boundaries [17]. This concept has been developed as grain boundary engineering (GBE) by Palumbo [18–23]. The feasibility of GBE has been demonstrated mainly by thermomechanical treatments, which can be broadly divided into strain annealing and strain recrystallization processes [20–30] based on process parameters, i.e. pre-strain and temperature. Palumbo et al. have improved the intergranular corrosion susceptibility in nickel base alloys by the strain recrystallization process [16,18,20,31], while King et al. have reported evolution of the GBCD in Cu by the strain annealing process [26,28]. However, the process parameters in the thermomechanical treatment differ between researchers, and the effects of process parameters on the GBCD during GBE are as yet unclear. Generation of  $\Sigma 3$  CSL boundaries by twin events [31] during thermomechanical treatment can increase the frequency of CSL boundaries in the materials, but may not always result in the optimum GBCD. Therefore, the purpose of this study was to optimize the parameters in thermomechanical treatment to achieve favorable GBCD and strong intergranular corrosion resistance in type 304 austenitic stainless steel by GBE.

## 2. Experimental procedure

The material used in this study was type 304 austenitic stainless steel. The chemical compo-

sition (wt%) is 18.28 Cr, 8.48 Ni, 0.60 Si, 1.00 Mn, 0.055 C, 0.029 P and 0.005 S. The initial size of the base material specimen was  $9 \times 10 \times 35 \text{ mm}^3$ . The specimens were solution-heat-treated at 1323 K for 0.5 h. Thermomechanical treatment was performed by cold-rolling and subsequent annealing. The roll reduction ratio in thickness as pre-strain was varied from 0 to 60%. The pre-strained specimens were annealed at various temperatures from 1200 to 1600 K and quenched in cold water. The GBCD was examined by orientation imaging microscopy (OIM). In this study, grain boundaries with  $\Sigma \leq 29$  were regarded as low- $\Sigma$  CSL boundaries, and Brandon’s criterion [32] was adopted for the critical deviation in the grain boundary characterization [9,33]. The intergranular corrosion resistance was evaluated by a double loop electrochemical potentiokinetic reactivation (DL-EPR) test [34] after sensitization treatment at 923 K for 1 or 5 h. The base material (BM) and 5% strain-annealed (r5%) specimens were assessed by a ferric sulfate-sulfuric acid test [35] after sensitization at 923 K for 2 h. The tested specimens were observed by scanning electron microscopy (SEM).

## 3. Results and discussion

### 3.1. Effect of pre-strain

Fig. 1 shows the effect of the roll reduction ratio as pre-strain on the reactivation current ratio during the DL-EPR test after sensitization treatment for 1 and 5 h, indicated by solid and open symbols, respectively. Each thermomechanically treated specimen except for the BM was annealed at 1300 K for 0.5 h after cold-rolling. As the degree of sensitization (DOS) is indicated by the reactivation current ratio, a lower current ratio means smaller sensitization. For 1-h sensitization, the DOS of the thermomechanically treated specimen was reduced compared with the value of the BM, and the minimum DOS was seen at 5% reduction. For 5-h sensitization, the 5% reduction also showed the minimum DOS, which is lower only than that of the BM.

OIM observations of the thermomechanically

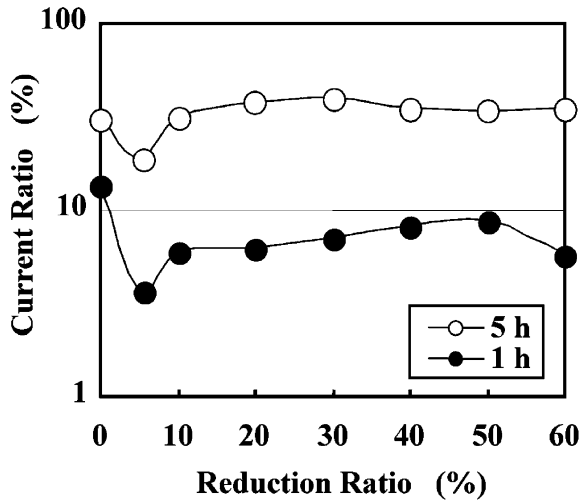


Fig. 1. The effect of roll reduction (0–60%) on the reactivation current ratio during the DL-EPR test after sensitization treatment for 1 and 5 h, indicated by solid and open symbols, respectively.

treated specimens showed the effect of the roll reduction ratio on the frequency of CSL boundaries (Fig. 2). The maximum at 5% reduction of the frequency of CSL boundaries is consistent with the minimum DOS at 5% reduction in Fig. 1, consider-

ing that higher CSL frequency leads to higher corrosion resistance.

Since Figs. 1 and 2 showed that a small strain around 5% in the thermomechanical treatment resulted in a minimum DOS during the DL-EPR test and a maximum in the frequency of CSL boundaries, the optimum degree of pre-strain around 5% was examined by varying roll-reduction in small steps within 10% as shown in Figs. 3 and 4. The specimens received an anneal at 1300 K for 0.5 h after cold rolling as in Figs. 1 and 2. The DOS decreased with an increase in the reduction ratio and showed a minimum at 5% reduction (Fig. 3). Correspondingly, the frequency of CSL boundaries indicated a maximum at 5% in the variations of the reduction ratio as shown in Fig. 4. Figs. 3 and 4 confirm an optimum pre-strain of 5% in strain annealing at 1300 K in the GBE process of this material.

In consideration of intergranular corrosion propagation, the GBCD in the material is as important as the frequency of CSL boundaries. Fig. 5 shows the GBCDs by OIM in the BM and the 5% strain-annealed specimen (r5%–1300 K–0.5 h) which indicated a maximum in the frequency of CSL boundaries during the thermomechanical

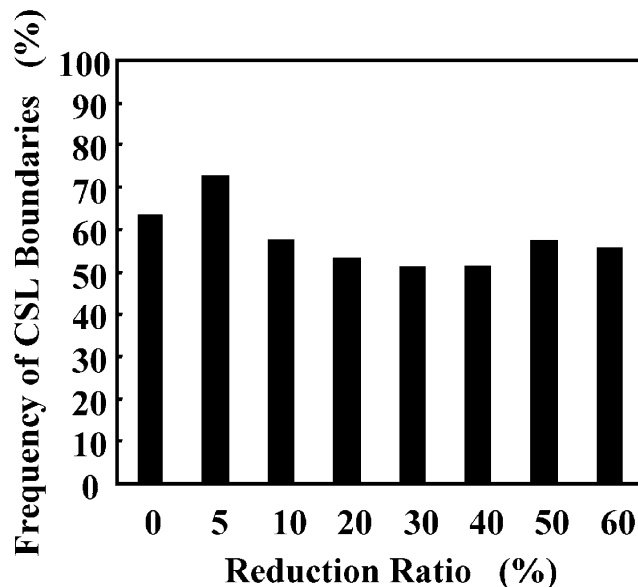


Fig. 2. The effect of roll reduction (0–60%) on the frequency of CSL boundaries.

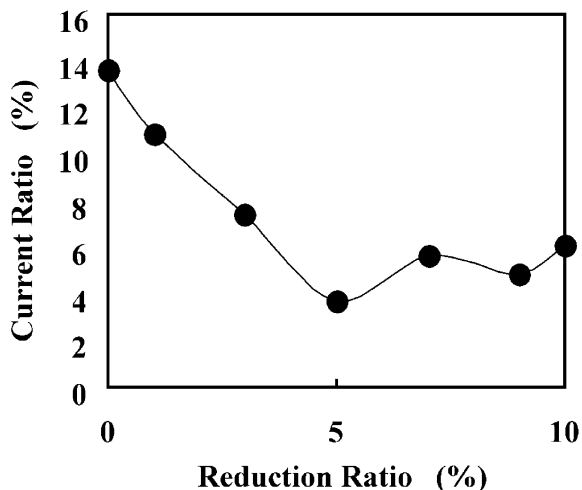


Fig. 3. The effect of roll reduction (0–10%) on the reactivation current ratio during the DL-EPR test after sensitization treatment for 1 h.

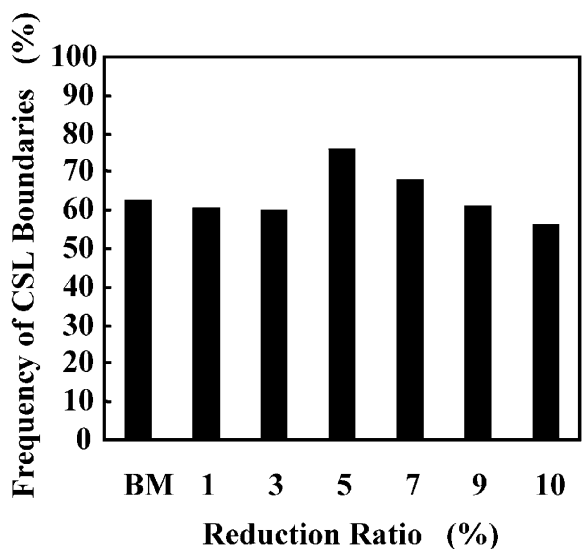


Fig. 4. The effect of roll reduction (0–10%) on the frequency of CSL boundaries.

treatment at 1300 K. Random and CSL boundaries are indicated by thick black and thin gray lines, respectively, in the upper panels (a), (b) and (c) of Fig. 5. The lower panels (a'), (b') and (c') of Fig. 5 show only the lines of random boundaries in the upper panels (a), (b), (c) of Fig. 5, respectively. A continuous network of random boundaries uni-

formly developed in the BM where the frequency of CSL boundaries is about 63%. The r5%–1300 K–0.5 h specimen had an average frequency of CSL boundaries of about 75%, but the GBCD was heterogeneous, i.e. areas with high (about 85%) and low (about 67%) frequencies of CSL boundaries coexisted in the specimen as shown in Fig. 5(b') and (c'), respectively. The continuation of the random boundary network was disrupted in the high CSL frequency areas (Fig. 5(b')), even though the CSL boundary frequencies in the other areas in the r5%–1300 K–0.5 h specimen were not very different from that in the BM. Intergranular corrosion tends to preferentially attack random grain boundaries because of selective chromium depletion due to chromium carbide precipitation at random boundaries in austenitic stainless steels [9,14]. If the higher CSL frequency area in the r5%–1300 K–0.5 h specimen were to spread thoroughly throughout the specimen, more significant improvement in intergranular corrosion resistance could be expected. An optimization of the GBCD was attempted to produce a more discontinuous random boundary network and a higher frequency of CSL boundaries in the next section.

### 3.2. Optimization of GBCD

The effect of annealing temperature at 5% pre-strain on the GBCD was examined by OIM. The annealing temperature and time were varied to find the process parameters needed to achieve the optimum GBCD. Annealing at 1400 K and higher temperatures did not result in any better differences in GBCD compared with that at 1300 K, but a favorable change in GBCD was observed during annealing at 1200 K, i.e. with increase in the annealing time at 1200 K, a high CSL frequency layer (about 85% CSL) was formed near the rolled surface and expanded into the specimen. Fig. 6 shows the developing front of the high CSL frequency layer at about 2 mm from the surface of the specimen annealed at 1200 K for 48 h, where the OIM indicates that the continuous random boundary network remained in the left side and that the high CSL frequency area including random boundary debris remained in the right side. A uniform distribution of the high CSL frequency area

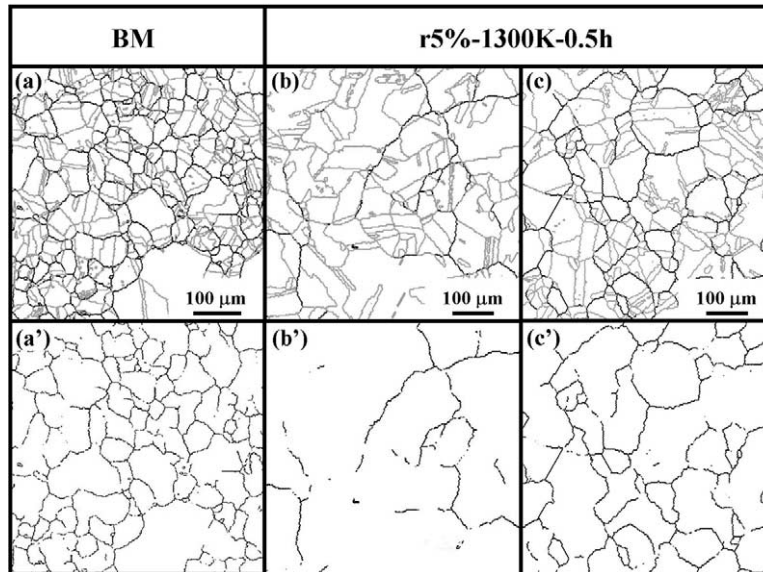


Fig. 5. GBCDs shown by OIM images for BM (a) and r5%–1300 K–0.5 h (b, c). Random and CSL boundaries are indicated by thick black and thin gray lines, respectively, in (a), (b) and (c), while only random boundaries are indicated in (a'), (b') and (c').

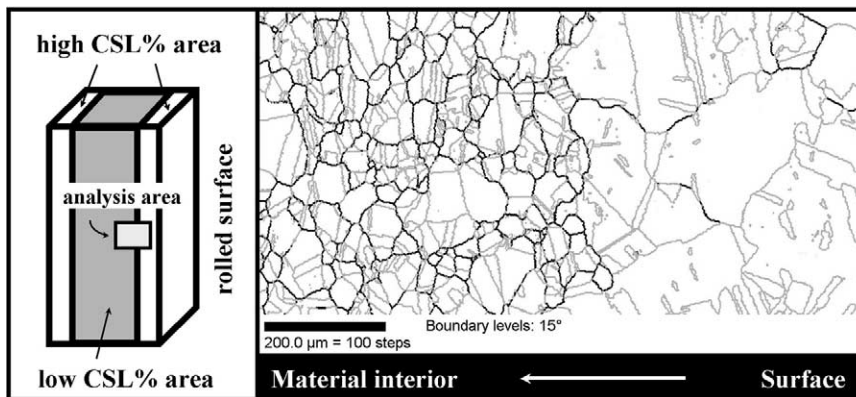


Fig. 6. GBCD by OIM in the border area at the front of the high CSL frequency layer in the r5%–1200 K–48 h specimen.

was achieved in the r5% specimen annealed at 1200 K for 72 h (r5%–1200 K–72 h), as shown in Fig. 7. The frequency of CSL boundaries was 86.5% homogeneously in the specimen with a thickness of about 10 mm. Some of the areas surrounded by random boundaries are larger than 0.5 mm as presumed from Fig. 7(b). A number of twins formed in the growing grains compensate grain-coarsening. Actually, the average grain size included twin boundaries in Fig. 7(a) is 31  $\mu\text{m}$  whereas that in the BM is 16  $\mu\text{m}$ . The network

of random grain boundaries in the BM was totally disrupted, and short random boundary segments were isolated in the r5%–1200 K–72 h specimen as shown in Fig. 7. The differences in GBCD between the BM, r5%–1300 K–0.5 h, r5%–1200 K–48 h and the r5%–1200 K–72 h specimens are schematically illustrated in Fig. 8.

Kumar et al. [29] attained a discontinuous network of random boundaries in a nickel alloy using more than three cycles of different thermomechanical processes including strain recrystallization,

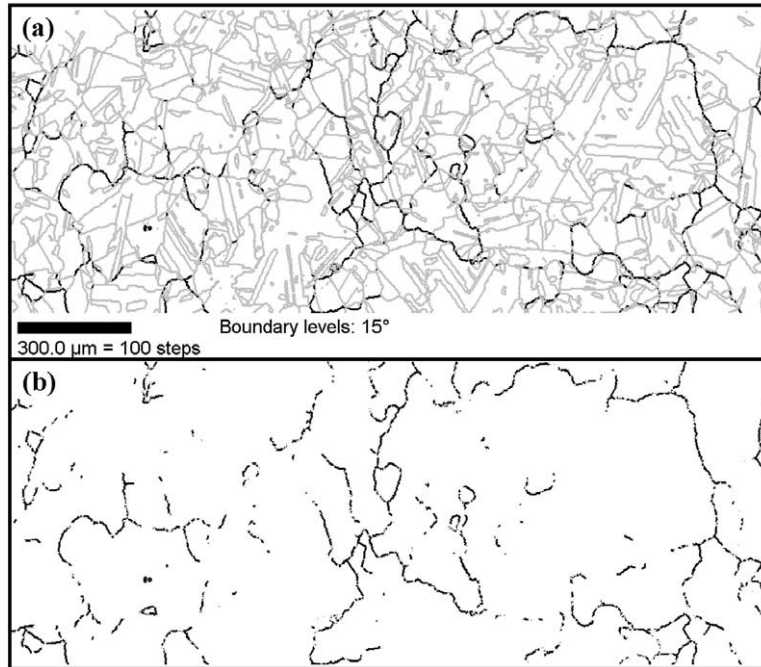


Fig. 7. Optimized GBCD in the r5%–1200 K–72 h specimen. Random and CSL boundaries are indicated by thick black and thin gray lines, respectively, in (a), while only random boundaries are indicated in (b).

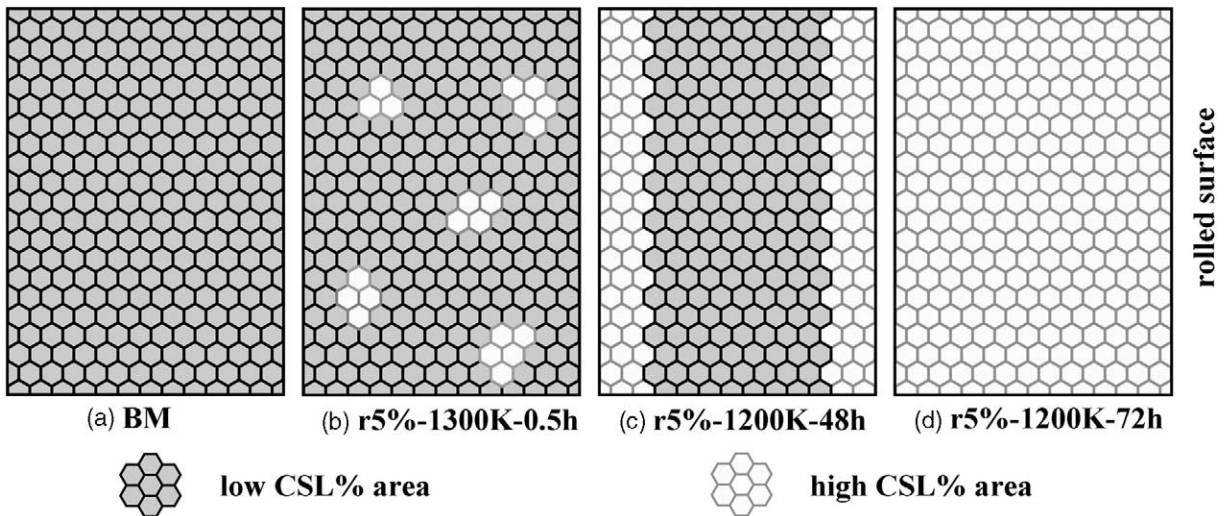


Fig. 8. Schematic illustrations of the GBCDs in the BM (a), r5%–1300 K–0.5 h (b), r5%–1200 K–48 h (c) and the r5%–1200 K–72 h (d) specimens.

while a similar GBCD was obtained in a 304 stainless steel by a single strain annealing process in the present study.

### 3.3. Intergranular corrosion resistance of optimized GBCD

The DL-EPR test results as shown in Figs. 1 and 3 reflect the fractional area of chromium depletion near sensitized grain boundaries on the test surface. The actual intergranular corrosion propagates along grain boundaries from the surface into the material and causes mass-loss due to grain dropping. The corrosion (mass loss) rate during the ferric sulfate-sulfuric acid test is shown for the BM, r5%–1300 K and r5%–1200 K specimens after sensitization in Fig. 9. The strain-annealed specimens have much lower corrosion rates than the BM for every test duration. The difference in mass-loss is much more than that expected simply from differences in DL-EPR test results and CSL boundary frequencies in Figs. 1–4, because the improvement in GBCD can strongly affect the mass-loss. The r5%–1200 K–72 h specimen with the optimized GBCD (Fig. 8(d)) indicated the smallest corrosion rate, which is less than one-fourth that of the BM, and less than half that of the r5%–1300 K–0.5 h specimen. The corrosion rate of the r5%–1200 K–48 h specimen with high CSL frequency layers (Fig. 8(c)) is higher than that of the r5%–1200 K–

72 h specimen with a uniformly high CSL frequency (Fig. 8(d)), but smaller than that of the r5%–1300 K–0.5 h specimen with randomly distributed high CSL frequency areas (Fig. 8(b)).

The surfaces (Fig. 10(a)) and cross-sections (perpendicular to the surface) (Fig. 10(b)) of the BM, r5%–1300 K–0.5 h and r5%–1200 K–72 h specimens after the ferric sulfate-sulfuric acid test were observed by SEM and are presented in Fig. 10. The surface appearances reveal that the grain dropping due to intergranular corrosion was depressed in the strain-annealed specimens, especially in the r5%–1200 K–72 h specimen with the optimized GBCD. The cross-sectional views also indicate that the penetration of intergranular corrosion from the surface into the interior of the material was arrested in the strain-annealed specimens, especially in the r5%–1200 K–72 h specimen with the optimized GBCD. These results verify that the optimum GBCD involving the homogeneously distributed high CSL frequency and the consequent discontinuous distribution of random boundaries can create a high resistance to intergranular corrosion in the material.

### 3.4. Evolution of the optimum GBCD

After DL-EPR and ferric sulfate-sulfuric acid tests, non-corroded parts in the corroded grain boundaries from where annealing twins were emitted were frequently observed in strain-annealed specimens as shown in Fig. 11(a) and (b). The OIM images in Fig. 11(a') and (b') suggest that the non-corroded parts in Fig. 11(a) and (b) transformed the grain boundary structures from random to  $\Sigma 9$  and  $\Sigma 29a$  CSL, respectively, by the emission of twin. OIM observations of strain-annealed specimens revealed that some but not all of the non-corroded parts in the corroded random boundaries were of low- $\Sigma$  CSL misorientations. Since an annealing twin formation generally reduces the grain boundary energy during grain growth [36], the grain boundary energy of the part where the twin was emitted is likely to be lower than that of the initial random boundary. Formation of a twin can introduce a low energy segment into the random high angle grain boundary and can sometimes result in low- $\Sigma$  CSL structures as shown in Fig.

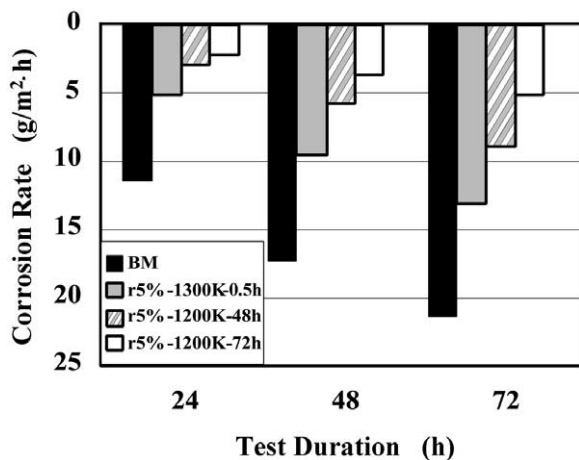


Fig. 9. The corrosion mass-loss of the BM and the strain-annealed specimens during the ferric sulfate-sulfuric acid test.

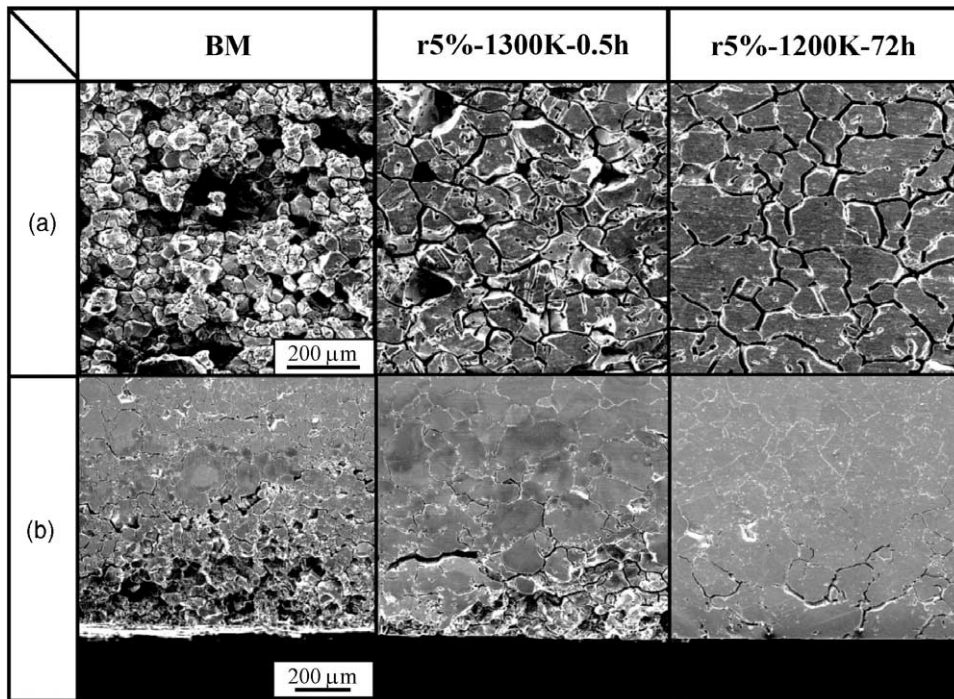


Fig. 10. The surfaces (a) and cross-sections (b) of the BM and the strain-annealed specimens after the ferric sulfate-sulfuric acid test.

11. Active twin events and reactions increase the frequency of CSL boundaries and also frequently produce low energy segments in high energy boundaries locally during thermomechanical treatment of low stacking fault energy materials such as 304 austenitic stainless steel. Well-distributed low energy segments in the grain boundary network create a discontinuous chain of chromium depletion and can arrest the percolation of intergranular corrosion from the surface, as illustrated in Fig. 12. A small pre-strain of around 5% is probably more suitable for an optimum distribution of non-corrosive segments than large pre-strains, because a large pre-strain tends to promote recrystallization which generates corrosive random boundaries and also CSL boundaries while a small pre-strain accelerates grain growth accompanying twins without generation of new random boundaries during thermomechanical treatment.

The evolution of the optimized GBCD during the strain annealing at 1200 K can be presumed in the following way. The small pre-strain activates

grain boundary migration without new grain generation. A migrating grain boundary inevitably interacts with lattice dislocations and other grain boundaries during grain growth. Because of the reactions, a low energy boundary cannot move a long distance, because the absorption rate of lattice dislocation by a low energy boundary is much lower than that of a random boundary [37] and the migration never occurs before completion of the absorption [38]. Also, the reactions possibly change the grain boundary structures to lower energy ones at high temperatures [39]. A low energy structure is stable and resistant to interactions with defects [40]. Therefore, a low energy boundary tends not to move, while a high energy boundary can migrate widely and consequently has a great opportunity for interaction with other boundaries or twin emissions so as to produce new low energy segments. Once low energy boundary segments are produced, they tend to survive for a long time. In the strain annealing at 1200 K, the small strain introduced by rolling promotes grain

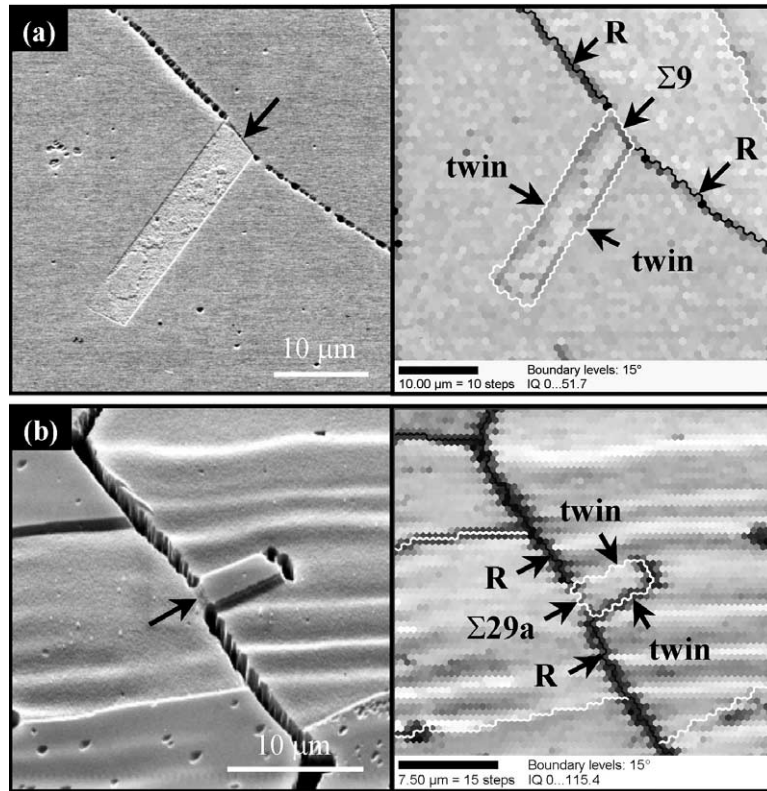


Fig. 11. Annealing twins at random boundaries shown by SEM and OIM. Random boundaries were partially transformed by twin emission to  $\Sigma 9$  (a) and  $\Sigma 29a$  CSL structures (b).

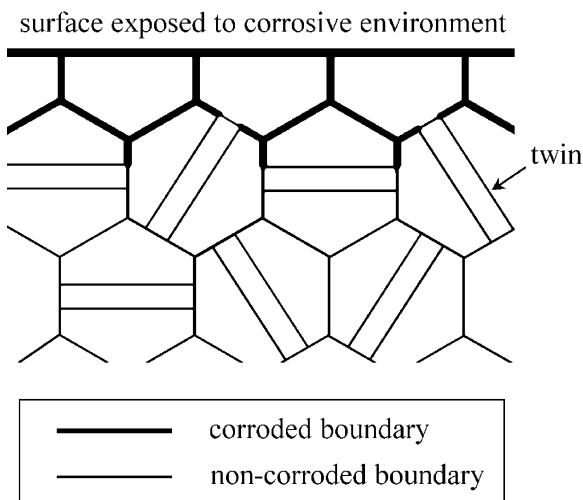


Fig. 12. Arrest of percolation of intergranular corrosion from the surface by distributed low energy segments.

growth and subsequently preferentially initiates the high CSL frequency layer near the specimen surface, and the layer grows into the specimen interior inversely along the strain gradient. Yoon and co-workers [41–44] have reported the transition between normal and abnormal grain growth in many metals and alloys related to grain boundary faceting during annealing. Abnormal grain growth at a relatively low temperature of 1200 K may also play a very important role in the evolution of optimized GBCD, because a small number of random boundaries migrate widely for a long time and interact effectively with other boundaries. On the other hand, normal grain growth at 1300 K and higher temperatures cannot effectively disrupt the random boundary network, because of the simultaneous, short migration of many random boundaries.

#### 4. Conclusion

Slight pre-strain annealing at a relatively low temperature for long time in thermomechanical treatment resulted in excellent resistance to intergranular corrosion of 304 stainless steel during DL-EPR and ferric sulfate-sulfuric acid tests. The high intergranular corrosion resistance resulted from an optimum GBCD which is described as a uniform distribution of a high frequency of CSL boundaries and consequent discontinuity of the random boundary network in the material. The optimum GBCD evolved due to expansion of a high CSL frequency layer nucleated near the rolled surface into the material interior. Such a high CSL frequency layer can be formed by introduction of low energy segments on migrating random boundaries during twin emission and boundary–boundary reactions in the grain growth without generation of new random boundaries.

#### Acknowledgements

The partial support of this work by a Grant-in-Aid for COE (Center of Excellence) Research (No.11CE2003) and a Grant-in-Aid for Scientific Research (B) (No.12555193) from the Japanese Ministry of Education, Culture, Sports, Science and Technology, by the Nuclear Research Promotion Program from the Japan Atomic Energy Research Institute (JAERI) and by the Inter-Research Centers Cooperative Program (IRCP) ‘Study of Materials Design with Higher Performance through Microstructural Analysis and Control of Grain Boundary’ from the Japan Society for the Promotion of Science (JSPS) is gratefully acknowledged. The authors wish to thank to Professor Tadao Watanabe for his useful advice, and Mr Takayuki Inoguchi, Mr Toshiyuki Maeta, Mr Yuya Konno and Mr Akira Honda for their technical assistance.

#### References

- [1] Kauris I, Gust W. Fundamentals of grain and interphase boundary diffusion. Stuttgart, Germany: Ziegler Press, 1988 [p. 275].
- [2] Coze JLe, Biscondi M, Levy J, Goux C. Mem Sci Rev Metall 1973;70:397.
- [3] Coze JLe, Biscondi M. Can Metall Q 1974;13:59.
- [4] Froment M. J Phys 1975;36:c4–371.
- [5] Qian XR, Chou YT. Philos Mag A 1982;45:1075.
- [6] Pumphrey PH. In: Chadwick GA, Smith DA, editors. Special high angle boundaries, grain boundary structure and properties. London: Academic Press; 1976. p. 13-9.
- [7] Palumbo G, Aust KT. Acta metall mater 1990;38:2343.
- [8] Lin P, Palumbo G, Erb U, Aust KT. Scripta metall mater 1995;33:1387.
- [9] Kokawa H, Shimada M, Sato YS. JOM 2000;34:52–7.
- [10] Kokawa H, Koyanagawa T, Shimada M, Sato YS, Kuwana T. In: Meike A, editor. Properties of complex inorganic solids 2. New York: Kluwer Academic/Plenum; 2000. p. 1-7.
- [11] Stickler R, Vinckier. Mem Sci Rev Metall 1963;60:489.
- [12] Číhal V, Kačová I. Corros Sci 1970;10:875.
- [13] Trillo EA, Murr LE. J Mater Sci 1998;33:1263.
- [14] Trillo EA, Murr LE. Acta mater 1999;47:235.
- [15] Palumbo G, Aust KT. J Phys 1988;49:C5–569.
- [16] Lehockey EM, Palumbo G, Lin P, Brennenstuhl AM. Scripta mater 1997;36:1211.
- [17] Watanabe T. Res Mechanica 1984;11:47.
- [18] Palumbo G, Lehockey EM, Lin P. JOM 1998;40:50–2.
- [19] Cheung C, Erb U, Palumbo G. Mater Sci Eng 1994;A185:39.
- [20] Lehockey EM, Palumbo G, Lin P. Metall Mater Trans A 1998;29A:3069.
- [21] Palumbo G. US Patent No. 5,702,543; 1997.
- [22] Palumbo G. US Patent No. 5,817,193; 1998.
- [23] Aust KT. Can Metall Q 1994;33:265.
- [24] Palumbo G, Aust KT. In: Chandra T, editor. Recrystallization 90. Warrendale, PA: TMS-AIME; 1990. p. 10-1.
- [25] Thomson CB, Randle V. J Mater Sci 1997;32:1909.
- [26] King WE, Schwartz AJ. Scripta mater 1998;38:449.
- [27] Thaveeprungsriporn V, Sinsrok P, Thong-Aram D. Scripta mater 2001;44:67.
- [28] Schwartz AJ, King WE. JOM 1998;50:50–2.
- [29] Kumar M, King WE, Schwartz AJ. Acta mater 2000;48:2081.
- [30] Randle V. Acta mater 1999;47:4187.
- [31] Lin P, Palumbo G, Aust KT. Scripta mater 1997;36:1145.
- [32] Brandon DG. Acta metall 1966;14:1479.
- [33] Kokawa H, Watanabe T, Karashima S. Scripta metall 1987;21:839.
- [34] Majidi AP, Streicher MA. Corrosion 1984;40:584.
- [35] Lee JB. Corrosion 1983;39:469.
- [36] Fullman RL, Fisher JC. J Appl Phys 1951;22:1350.
- [37] Kokawa H, Watanabe T, Karashima S. J Mater Sci 1983;18:1183.
- [38] Pumphrey PH, Gleiter H. Philos Mag 1974;30:593.
- [39] Kokawa H, Watanabe T, Karashima S. Philos Mag A 1981;44:1239.
- [40] Kokawa H, Watanabe T, Karashima S. Scripta metall 1983;17:1155.
- [41] Lee SB, Yoon DY, Henry MF. Acta metall 2000;48:3071.

[42] Lee SB, Hwang NM, Yoon DY, Henry MF. Metall Mater Trans A 2000;31A:985.

[43] Koo JB, Yoon DY. Metall Mater Trans A 2001;32A:469.

[44] Choi JS, Yoon DY. ISIJ Int 2001;41:478.